

Effect of Loading Level and Span Length on Critical Buckling Load

Marwah A. Mohsen
 Department of Civil Engineering
 University of Basrah
 marwahalfartusy@yahoo.com

Dr. Abdalnassre M. Abbas
 Department of Civil Engineering
 University of Basrah
 Nasser21272@gmail.com

Dr. Ahmed S. Saadoon
 Department of Civil Engineering
 University of Basrah
 ahmsag@gmail.com

Abstract: An investigation was conducted to study the effect of loading level with respect to shear center and span length on lateral torsional buckling of steel I-section beams using linear and nonlinear finite element analysis available in ANSYS (version 12.0) computer program. The steel beams which have been studied included prismatic beams and linearly web-tapered beams with web tapering ratio of (0.5). The maximum height of all beams was 300 mm with span length of 4, 6 and 8 m. The critical buckling loads for prismatic and linearly tapered cantilever and simply supported beams subjected to point load and uniformly distributed load were determined. The results showed that, the bottom flange loading gives a buckling loads higher than that of the top flange loading with percentage increases of 148% and 155% for the linear and nonlinear analysis respectively for the prismatic beams. While for the tapered beams, these percentages increases were 61% and 67% respectively.

I. INTRODUCTION

If the flexural rigidity of the beam in the plane of the web is many times greater than its lateral rigidity, the beam may buckle and collapse long before the bending stresses due to the transverse load reach the yield point [1]. In case of slender beams, which having narrow sections with narrow flanges and long spans, these beams lack both lateral flexural rigidity and torsional rigidity, and if left unrestrained, they may buckle by combined twist and lateral bending of the cross-section. This phenomenon is known as lateral torsional buckling of beams. The lowest load at which this critical condition occurs represents the critical load for the beam [2].

Yuen [3], in 1998, presented a study consists of an experimental and analytical investigation of the lateral buckling behavior of steel I-section girders braced by continuous or discrete U-frames. Twin I-section girders have been used in the test and the lateral deflection of the compression flanges and final buckling modes were recorded and the coupling effect of U-frame action is clearly demonstrated. Using a large displacement elasto-plastic finite elements package, ABAQUS (version 4.7), finite elements idealizations of the tests were established and analyzed. Good correlation between the experiments and the numerical analyses was reached.

Simpson [4], in 2000, presented an analytical investigation of the behavior of curved steel girders. He studied a popular type of curved bridge consists of steel I-girders interconnected by cross-frames and a composite concrete deck slab. Prior to hardening of the concrete deck each I-girder is susceptible to a lateral torsional buckling-type failure. Unlike a straight I-girder, a curved I-girder resists major components of stress resulting from strong axis bending, weak axis bending, and warping. The combination of these stresses reduces the available strength of a curved girder versus that of an equivalent straight girder. This study included a nonlinear modeling of curved steel girders. This is accomplished by incorporating large deflection and nonlinear material behavior into three dimensional finite elements models generated using the program ANSYS (version 5.0, 5.2, and 5.3).

II. MODELING AND IDEALIZATION OF STEEL BEAMS

Stress-strain diagrams present valuable information necessary to understand how steel will behave in a given situation [3]. Thus, this relation between stresses and strains of a structure is of an importance in modeling any structural problem so that this modeling will be able to represent realistically the response of the material and the behavior of the structure according to. In this study, the steel material has been modeled as Von Mises material with isotropic hardening.

The stress-strain curve [5] of steel is idealized as a bilinear curve, representing elastic-plastic behavior with strain hardening. This curve is assumed to be identical in tension and compression as shown in figure (1). Material properties for steel beams as follows:

Elastic modulus $E_{s1} = 210000 \text{ N/mm}^2$.

Poisson's ratio $\nu = 0.3$.

Yield stress $f_y = 350 \text{ N/mm}^2$.

Strain hardening modulus E_{s2} is assumed to be $0.1 E_{s1}$.

In this study shell element, (SHELL63) [6], was used to model the steel beam. This element is defined by four nodes having six degrees of freedom at each node: translations in x, y, and z directions and rotations about the nodal x, y, and z axes. The geometry, node locations, and the coordinate system for this element are shown in figure (2).

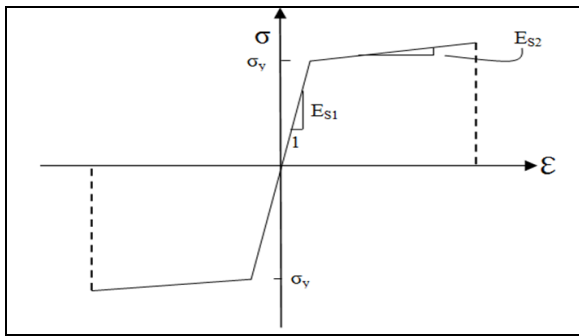


Figure 1 Typical Stress-Strain Curve for Steel[5]

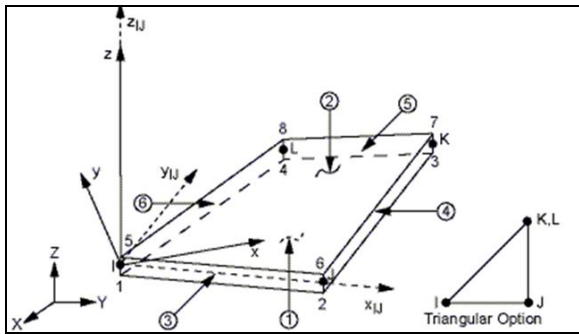


Figure 2 SHELL63 Geometry[6]

III. BUCKLING ANALYSIS

Buckling analysis is a technique used to determine buckling loads; the critical loads at which a structure becomes unstable, and the different ways that the structural member can deform which known as buckling mode shapes. Two techniques are available in ANSYS program for predicting the buckling load and buckling mode shapes: eigenvalue (linear) buckling analysis and nonlinear buckling analysis. Because the two methods can yield different results, it is necessary first to understand the differences between them.

A. Eigenvalue (Linear) Buckling Analysis

Eigenvalue buckling analysis predicts the theoretical buckling strength of an ideal linear elastic structure. This method corresponds to the textbook approach to elastic buckling analysis. However, imperfections and nonlinearities prevent most real-world structures from achieving their theoretical elastic buckling strength. Thus, eigenvalue buckling analysis often yields un-conservative results, and should generally not be used in actual day-to-day engineering analysis.

B. Nonlinear Buckling Analysis

Nonlinear buckling analysis is usually the more accurate approach and is therefore recommended for design or evaluation of actual structures. This technique employs a nonlinear static analysis with gradually increasing loads to seek the load level at which the structure becomes unstable. Using the nonlinear technique, the model can include features such as initial imperfections, plastic behavior, gaps, and large-deflection response.

IV. NONLINEAR SOLUTION TECHNIQUES IN ANSYS

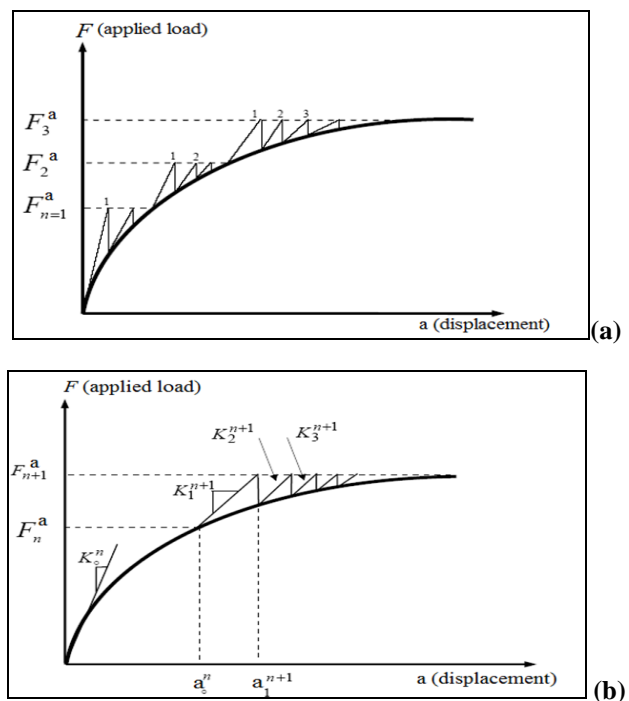
In the nonlinear analysis, solving the governing equations may be achieved by using three basic solution techniques. These are the incremental, iterative, and combined incremental-iterative approaches.

A. Incremental-Iterative Technique

This technique, as shown in figure (3-a), is usually carried out by applying the external loads as a sequence of sufficiently small increments, and within each increment of loading, iterations are performed until equilibrium is satisfied according to some selected convergence criterion. The incremental-iterative procedures comprise the following procedures:

B. Full Newton-Raphson Procedure

In this procedure, the stiffness matrix is updated at every equilibrium iteration, thus a large amount of computation may be required to form and solve the stiffness matrix, figure (3-b).

Figure 3 a) Incremental-Iterative Technique,
b) Full Newton-Raphson Method

V. CONVERGENCE CRITERION

A convergence criterion is required in order to terminate the iterative process required for solving the governing nonlinear equation, i.e., a termination criterion for iterative process should be used to stop the iteration when sufficient accuracy is achieved or when no further iterations are necessary. The ANSYS program gives a number of choices when designating a convergence criterion. The convergence criterion for the nonlinear analysis of structural problems can be classified as: Force

criterion, Displacement criterion and Stress criterion. The force criterion has been used in this study.

VI. DETAILS OF STUDIED BEAMS

In this study, the critical buckling loads for different types of prismatic and linearly web-tapered I-section beams were considered. Investigated beams having lengths of 4, 6, and 8m. The web-tapering ratio was considered to be 0.5, that is; $h_{min} = 0.5 h_{max}$. Table (1) gives the details for all beams which are considered in this study, and figure (4) shows the configuration of the considered beams.

VII. RESULTS OF BUCKLING ANALYSIS

A. Cantilever Beams under Point Load

The critical buckling loads Q_{cr} were determined for the two types of beams, the prismatic and linearly web-tapered cantilever beams given in table (1), and the results are listed in tables (2) to (5). The numerical results obtained by Andrade[7], which were calculated for the same beams by using the finite elements package ABAQUS (version 6.3), were also listed in these tables. A comparison between the results was made to verify the accuracy of the results of the used finite elements models in the present study. The comparison showed a good agreement, and that proved the ability and accuracy of the used models to predict the critical buckling loads in two different techniques (linear and nonlinear) and for complex cases such as linearly web-tapered steel beams. Tables (6) and (7) show a comparison between the obtained eigenvalue (linear) buckling loads $Q_{cr lin}$ and nonlinear buckling loads $Q_{cr nlin}$.

TABLE 1 DETAILS OF BEAMS

Beam item	L M	b_f mm	h_{max} mm	h_{min} mm	t_f mm	t_w mm	Description
PC4	4	150	300	300	10	6	Prismatic Cantilever
PC6	6	150	300	300	10	6	Prismatic Cantilever
PC8	8	150	300	300	10	6	Prismatic Cantilever
TC4	4	150	300	150	10	6	Web-Tapered Cantilever
TC6	6	150	300	150	10	6	Web-Tapered Cantilever
TC8	8	150	300	150	10	6	Web-Tapered Cantilever
TS4	4	150	300	150	10	6	Web-Tapered Simple beam
TS6	6	150	300	150	10	6	Web-Tapered Simple beam
TS8	8	150	300	150	10	6	Web-Tapered Simple beam

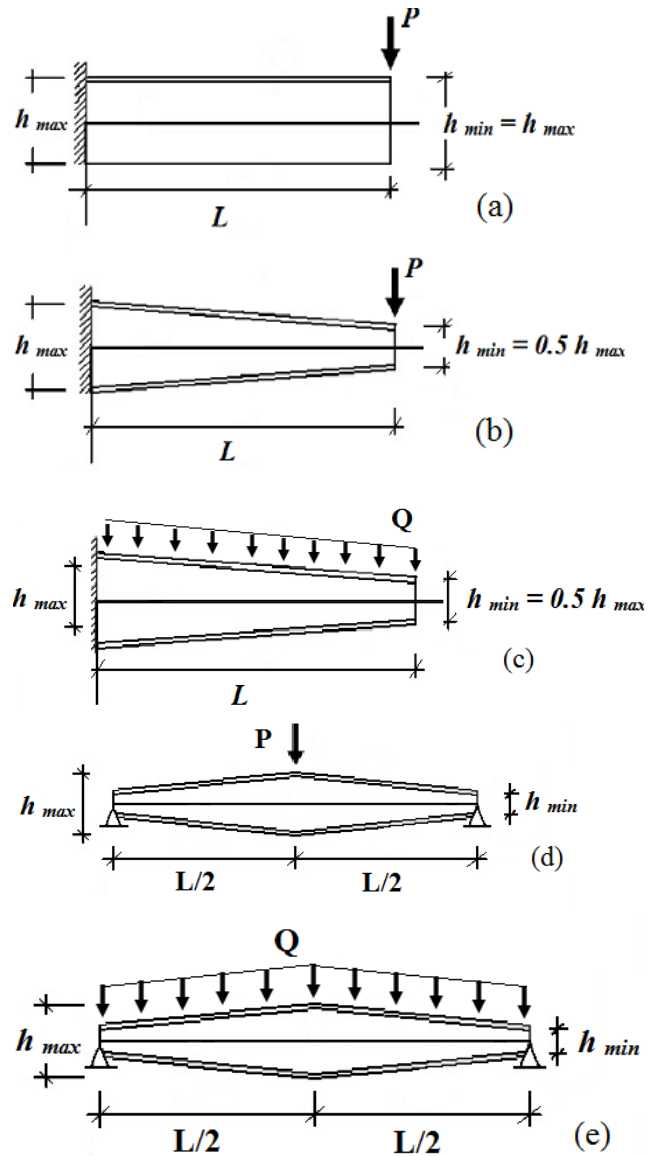


Figure 4 a) Prismatic Cantilever with Point Load, b) Web-Tapered Cantilever with Point Load, c) Web-Tapered Cantilever with UDL, d) Web-Tapered Simply Supported with Point Load, e) Web-Tapered Simply Supported with UDL[7]

TABLE 2 LINEAR CRITICAL BUCKLING LOADS OF PRISMATIC BEAMS UNDER POINT LOAD

Beam Item	Q_{cr} ANSYS kN	Q_{cr} ABAQUS kN	$\frac{Q_{crANS}}{Q_{crABA}}$	Loading level
PC4	24.86	22.80	1.09	Top flange loading
PC6	11.95	11.40	1.05	
PC8	7.06	6.90	1.02	
PC4	58.11	47.40	1.23	Centroidal loading
PC6	21.20	20.20	1.05	
PC8	10.53	10.40	1.01	
PC4	83.08	83.40	0.97	Bottom flange loading
PC6	27.32	27.40	0.98	
PC8	12.79	12.80	0.99	

TABLE 3 NONLINEAR CRITICAL BUCKLING LOADS OF PRISMATIC CANTILEVER BEAMS UNDER POINT LOAD

Beam Item	Q _{cr} ANSYS kN	Q _{cr} ABAQUS kN	$\frac{Q_{crANS}}{Q_{crABA}}$	Loading level
PC4	25.08	23.00	1.09	Top flange loading
PC6	12.11	11.50	1.05	
PC8	7.19	7.00	1.03	
PC4	60.28	48.60	1.24	Centroidal loading
PC6	21.98	20.90	1.05	
PC8	10.92	10.70	1.02	
PC4	86.82	87.20	0.99	Bottom flange loading
PC6	28.50	28.60	0.99	
PC8	13.33	13.40	0.99	

TABLE 4 LINEAR CRITICAL BUCKLING LOADS OF LINEARLY WEB-TAPERED CANTILEVER BEAMS UNDER POINT LOAD

Beam Item	Q _{cr} ANSYS kN	Q _{cr} ABAQUS kN	$\frac{Q_{crANS}}{Q_{crABA}}$	Loading level
TC4	35.19	31.60	1.11	Top flange loading
TC6	15.64	15.20	1.03	
TC8	8.53	8.40	1.01	
TC4	56.50	53.50	1.06	Centroidal loading
TC6	20.47	20.30	1.01	
TC8	10.29	10.20	1.01	
TC4	70.00	70.00	1.00	Bottom flange loading
TC6	23.70	23.70	1.00	
TC8	11.39	11.40	0.99	

TABLE 5 NONLINEAR CRITICAL BUCKLING LOADS OF LINEARLY WEB-TAPERED CANTILEVER BEAMS UNDER POINT LOAD

Beam Item	Q _{cr} ANSYS kN	Q _{cr} ABAQUS kN	$\frac{Q_{crANS}}{Q_{crABA}}$	Loading level
TC4	36.47	32.70	1.11	Top flange loading
TC6	16.45	15.90	1.03	
TC8	9.04	9.00	1.01	
TC4	60.09	57.60	1.04	Centroidal loading
TC6	22.02	21.80	1.01	
TC8	11.33	10.90	1.04	
TC4	75.90	76.10	0.99	Bottom flange loading
TC6	25.64	25.70	0.99	
TC8	12.49	12.30	0.99	

TABLE 6 LINEAR AND NONLINEAR CRITICAL BUCKLING LOADS OF PRISMATIC CANTILEVER BEAMS UNDER POINT LOAD

Beam Item	Q _{cr lin} (Linear) kN	Q _{cr nlin} (Nonlinear) kN	$\frac{Q_{cr lin}}{Q_{cr nlin}}$	Loading level
PC4	24.86	25.08	0.99	Top flange loading
PC6	11.95	12.11	0.99	
PC8	7.06	7.19	0.98	
PC4	58.11	60.28	0.96	Centroidal loading
PC6	21.20	21.98	0.97	
PC8	10.53	10.92	0.96	
PC4	83.08	86.82	0.96	Bottom flange loading
PC6	27.32	28.50	0.96	
PC8	12.79	13.33	0.96	

TABLE 7 LINEAR AND NONLINEAR CRITICAL BUCKLING LOADS OF WEB-TAPERED CANTILEVER BEAMS UNDER POINT LOAD

Beam Item	Q _{cr lin} (Linear) kN	Q _{cr nlin} (Nonlinear) kN	$\frac{Q_{cr lin}}{Q_{cr nlin}}$	Loading level
TC4	35.19	36.47	0.97	Top flange loading
TC6	15.64	16.45	0.95	
TC8	8.53	9.04	0.94	
TC4	56.50	60.09	0.94	Centroidal loading
TC6	20.47	22.02	0.93	
TC8	10.19	11.33	0.90	
TC4	70.00	75.90	0.92	Bottom flange loading
TC6	23.70	25.64	0.92	
TC8	11.39	12.49	0.91	

Figures (5) to (8) show the effect of the variation in length of the beams and level of the applied loads on the critical buckling loads. The load was applied at three different places of the cross-section; top flange, centroid, and bottom flange. From these figures, it can be seen that, for the same beam, the bottom flange loading case gives a buckling load greater than the other two cases. Also the top flange loading case gives a buckling load lesser than the other two cases. The results showed that, the bottom flange loading gives a buckling loads higher than that of the top flange loading with percentage increases of 148 and 155% from the linear and nonlinear analysis respectively, for the prismatic beams. While for the tapered beams, these percentages increases were 61 % and 67% respectively. The reason of this variation is related to the position of the applied load with respect to the shear centre. Double symmetric I-section, considered in this study, having a shear centre coincides with the centroid, and when the load applied at the centroid, its resultant will pass through the shear centre and any twisting of the cross-section will prevented. As the load applied above or below the shear centre, an additional torque, which equals the applied load multiplied by its arm from the shear centre, will introduced. The load applied above the shear centre increases the twisting of the beam and decreases the resistance to buckling, and conversely when the load applied below the shear centre. It is clear that, as the length of the beams increases, the critical buckling load decreases. This is due to the increase of slenderness ratio. Figures (9) to (11) shows the first buckling mode shapes for cantilever beams under end point load.

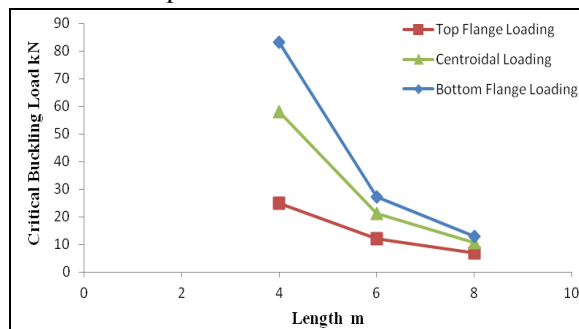


Figure 5 Effect of level of loading and length of beam on linear critical buckling loads for prismatic beams PC4, PC6 and PC8

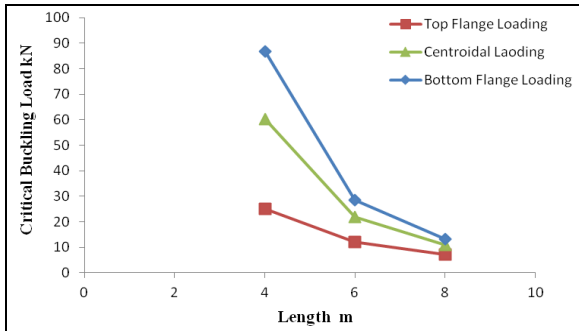


Figure 6 Effect of level of loading and length of beam on nonlinear critical buckling loads for prismatic beams PC4, PC6 and PC8

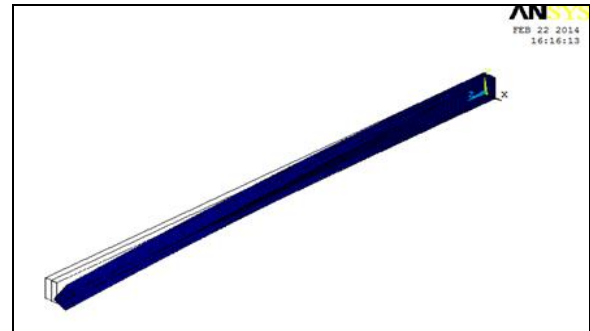


Figure 10 First Buckling Mode Shape for Beam PC6 under End Point Load (Centroidal Loading)

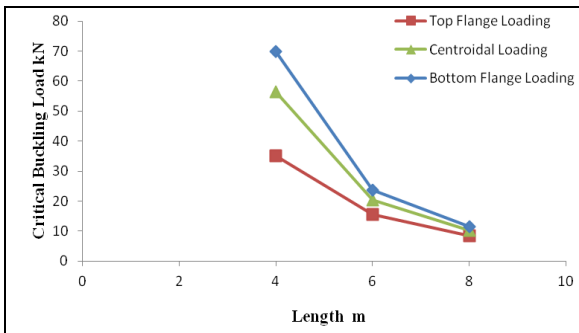


Figure 7 Effect of level of loading and length of beam on linear critical buckling loads of web-tapered beams TC4, TC6 and TC8

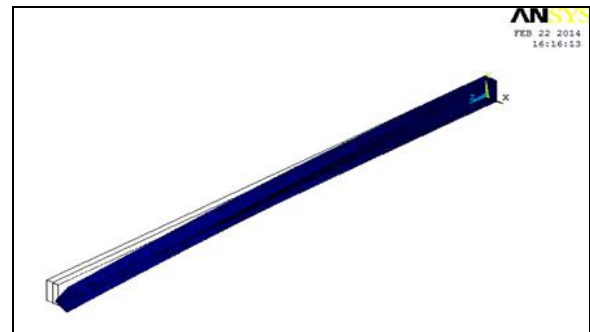


Figure 11 First Buckling Mode Shape for Beam PC8 under End Point Load (Bottom Flange Loading)

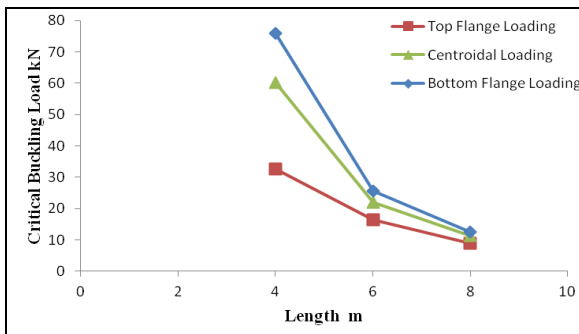


Figure 8 Effect of level of loading and length of beam on nonlinear critical buckling loads of web-tapered beams TC4, TC6 and TC8

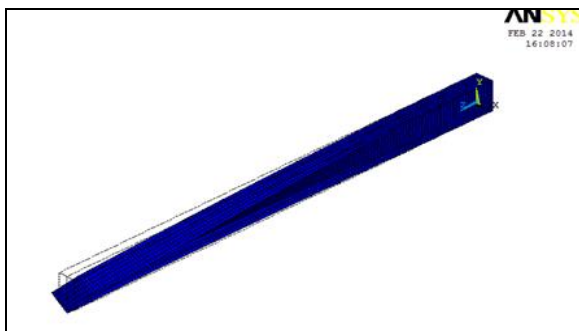


Figure 9 First Buckling Mode Shape for Beam PC4 under End Point Load (Top Flange Loading)

B. Cantilever Beams under Uniformly Distributed Load (UDL)

The critical buckling loads Q_{cr} , from the two analyses, were determined for linearly web-tapered cantilever beams with UDL, and listed in table (8). The resulted buckling loads from the two analyses with the effect of length variation are shown in figure (12). Approximately, the same values for the buckling loads were obtained. It is obvious that the critical buckling load, from the two analyses, decreases as the length of the beam increases. The percentage decrease in buckling loads with length varying from 4m to 8m is 88% from linear buckling analysis and 87.7% from nonlinear buckling analysis. Figure (13) shows the first buckling mode shape for beam TC4 under UDL.

TABLE 8 LINEAR AND NONLINEAR CRITICAL BUCKLING LOADS FOR LINEARLY WEB-TAPERED CANTILEVER BEAMS UNDER UDL

Beam item	Length m	$Q_{cr \text{ lin}}$ kN/m	$Q_{cr \text{ nlin}}$ kN/m	$\frac{Q_{cr \text{ lin}}}{Q_{cr \text{ nlin}}}$
TC4	4	28.26	28.95	0.98
TC6	6	8.32	8.61	0.97
TC8	8	3.40	3.55	0.95

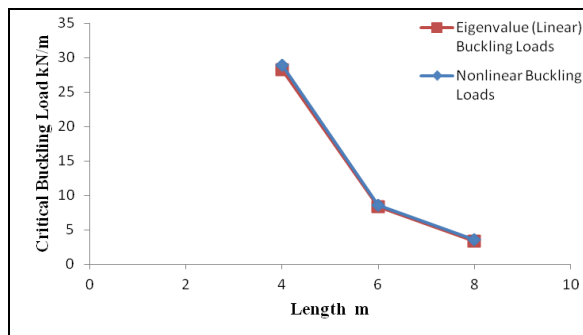


Figure 12 Critical buckling loads for web-tapered cantilever beams under UDL

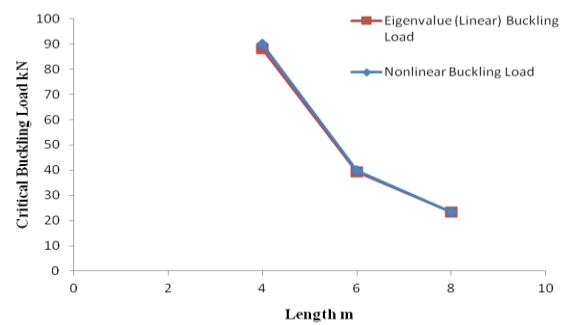


Figure 14 critical buckling loads for linearly web-tapered simply supported beams under point load

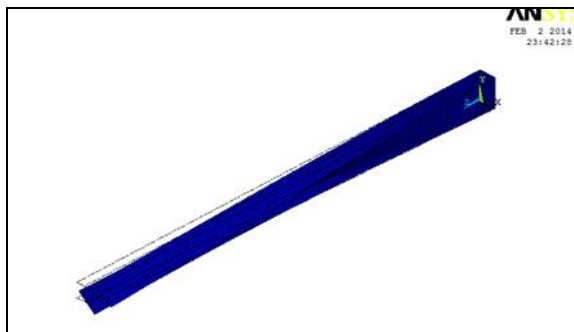


Figure 13 First Buckling Mode Shape for Beam TC4 under UDL

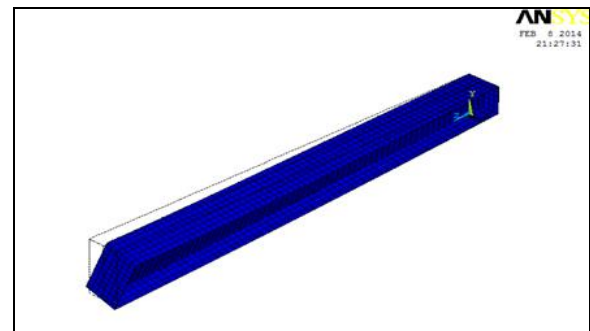


Figure 15 First Buckling Mode Shape for Half Span of Beam TS4 under Point Load

C. Simply Supported Beams under Point Load

The critical buckling loads Q_{cr} for linearly web-tapered simply supported beams subjected to point load at mid span were obtained. The critical buckling loads from the two analyses are listed in table (9), and the resulted buckling loads obtained with respect to the variation in length of the beam, are shown in figure (14). From this figure, it's apparent that the buckling capacity of the simply supported beam decreases as the length of this beam increases from 4m to 8m and the percentages decreases corresponding are 73.5% from linear buckling analysis and 74% from nonlinear buckling analysis. Also, a great proximity in the results of linear and nonlinear buckling analyses can be noticed. Figure (15) shows the first buckling mode shape for half Sspan of beam TS4 under point load.

TABLE 9 LINEAR AND NONLINEAR CRITICAL BUCKLING LOADS FOR LINEARLY WEB-TAPERED SIMPLY SUPPORTED BEAMS UNDER POINT LOAD

Beam item	Length m	$Q_{cr \text{ lin}}$ kN	$Q_{cr \text{ nlin}}$ kN	$\frac{Q_{cr \text{ lin}}}{Q_{cr \text{ nlin}}}$
TS4	4	88.08	89.94	0.98
TS6	6	39.42	39.86	0.99
TS8	8	23.32	23.36	0.99

D. Simply Supported Beams under Uniformly Distributed Load

The linear and nonlinear critical buckling loads Q_{cr} for linearly web-tapered simply supported beams loaded by UDL were determined, and the obtained results are listed in table (10). The resulted buckling loads from the two analyses are shown in figure (16) which shows a great proximity in the results of linear and nonlinear buckling analyses. Also it shows that, as it was noticed in the previous cases, the effect of the increasing the span length is against the buckling strength, and the percentage decreases are 93.5% and 86% from linear and nonlinear buckling analysis, respectively.

TABLE 10 LINEAR AND NONLINEAR CRITICAL BUCKLING LOADS FOR LINEARLY WEB-TAPERED SIMPLY SUPPORTED BEAMS UNDER UDL

Beam item	Length m	$Q_{cr \text{ lin}}$ kN/m	$Q_{cr \text{ nlin}}$ kN/m	$\frac{Q_{cr \text{ lin}}}{Q_{cr \text{ nlin}}}$
TS4	4	38.53	39.11	0.98
TS6	6	11.86	11.90	0.99
TS8	8	5.30	5.48	0.97

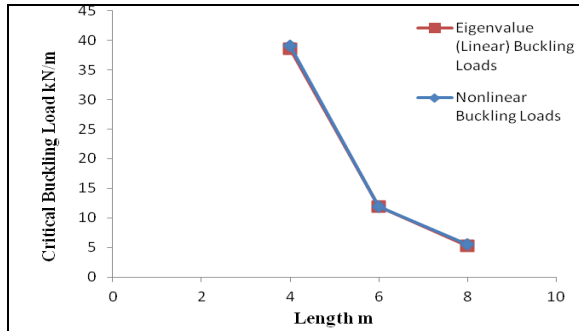


Figure 16 Critical buckling loads for linearly web-tapered simply supported beams under UDL

VIII. CONCLUSIONS

- 1- The results proved the ability and accuracy of the used models to predict the critical buckling loads in two different techniques (linear and nonlinear) and for complex cases such as linearly web-tapered steel beams.
- 2- The nonlinear analysis yielded buckling load values slightly greater than those resulted from the linear analysis. The ratio between the linear and nonlinear buckling loads was ranged from 0.95 to 0.99 for all loading cases.
- 3- As the length of the beams increases, the critical buckling load decreases due to the increase of slenderness ratio.
- 4- One of the most important factors that effecting the critical buckling loads for I-section beams is the load level relative to the shear centre. When the load is applied at the bottom flange the buckling resistance will increase and inversely when the load is applied at the top flange.
- 5- For cantilever beams loaded by a point load, the bottom flange loading gave a nonlinear buckling load greater than that of the top flange loading by (38% - 108%) and (85% - 246%) for the linearly web-tapered and prismatic beams, respectively. The smallest percentage is corresponding to the shortest span length.

IX. REFERENCES

- [1] Bleich, F., and Ramsey, L.B., "Buckling Strength of Metal Structures", McGRAW-Hill, New York, 1952, pp. 149.
- [2] Timoshenko, S.P., and Gere, J.M., "Theory of Elastic Stability", McGRAW-Hill, New York, 1961, pp. 251.
- [3] Yuen, R.M., "Lateral Buckling of Steel I-Section Bridge Girders Braced by U-Frames", Ph.D. Thesis, University of Leeds, October, 1992.
- [4] Simpson, M.D., "Analytical Investigation of Curved Steel Girder Behavior", Ph.D. Thesis, University of Toronto, 2000.
- [5] Smith, J.C., "Structural Steel Design (LRFD Approach)", Second Edition, John Wiley and Sons, 1996, USA.
- [6] ANSYS, "ANSYS Help", Release 12.0, ANSYS Inc. Canonsburg, April, 2009.
- [7] Andrade, A., Camotim, D., and Dinis, P.B., "Lateral-Torsional Buckling of Singly Symmetric Web-Tapered Thin-Walled I-Beams: 1D vs. Shell FEA", Computers and Structures, Elsevier, Vol. 85, 2007, pp. 1343-1359.